Tunable protein microlens array

Zhishan Hou (侯智善), Jiaji Cao (曹嘉冀), Aiwu Li (李爱武)*, and Han Yang (杨 罕)**

State Key Laboratory on Integrated Optoelectronics, College of Electronic Science and Engineering, Jilin University, Changchun 130012, China

**Corresponding author: liaw@jlu.edu.cn; **corresponding author: yanghan@jlu.edu.cn*

Received February 1, 2019; accepted March 14, 2019; posted online June 6, 2019

Based on natural protein materials, a series of lenses with different heights and focal lengths were assembled on glass substrates by femtosecond laser non-contact, masking, and cold processing. This lens array itself possesses unique and characteristic optical performance in three-dimensional parallel imaging and bending imaging. What is more profound is that by using equilibrium swelling of protein-hydrogel, once the lens array was placed in a liquid environment, with the change of ion concentration (e.g., pH), the refractive index and curvature of the protein-hydrogel would change, which leads to the flex of the focal plane of the lens, finally realizing the dynamical tunability of a protein microlens. These smart stress devices may have great potential in optical biosensing and microfluidic chip integration fields.

OCIS codes: 170.1420, 230.3990.
doi: 10.3788/COL201917.061702.

Since the 21st century, micro-optics devices have been studied and received considerable in-depth attention in modern industry[1,2]. Among them, as a kind of typical micro-optics device, the microlens and microlens array (MLA) have unique advantages, such as light weight, small size, ease of integration, stable performance, large number of quantitative production, and low power consumption[3]; they are playing an important role in optical information processing[4], beam shaping[5], optical interconnect[6], three-dimensional (3D) imaging[7], and bionic compound eye[8]. For example, Zheng *et al.* used an MLA based on ion wind patterning to improve the low light extraction efficiency (LEE) of chip-on-board (COB) packaging light-emitting diodes (LEDs)[9]. On this basis, the microlens imitates the structure and working mode of human eyes, realizing variable focus by changing the interface curvature or refractive index of the lens material. At present, the varifocal microlens mainly includes three types based on (1) the phenomenon electrowetting principle[10], (2) the polymer-dispersed liquid crystal[9–12], and (3) the liquid-filled technique[13]. However, the theoretical and experimental studies in varifocal MLA areas are rarely reported, especially for those that are based on biocompatibility and can be applied to organisms.

We have successfully prepared protein-based tunable lenses, but have not fully utilized the material and structural characteristics for more functional devices and applications[14]. Therefore, in this Letter, we report on a protein-hydrogel-based MLA with different curvature unit lenses (PMLADC) by using facile and rapid maskless femtosecond laser direct writing (FsLDW). Through the ultra-precise custom processing by FsLDW[15–22], the sizes of the unit lenses are different and precisely controlled along with their positions. Such special structural prototypes will give the PMLADC high potential in numerous areas, such as curvature correction[23], and show great attraction in a real-time 3D imaging system[24]. Significantly, due to the use of natural proteins as the basic building block, with low thermal damage of the femtosecond laser, the PMLADC's unique pH response and good biocompatibility bring great promise to optical and biomedical applications, such as 3D dynamic measurement in complex organisms.

Herein, commercial bovine serum albumin (BSA; 600 mg/mL in aqueous solution) and photosensitizer (Rhodamine B, RhB, 2 mg/mL) were used to prepare 3D protein-based optical micro-devices. A femtosecond laser beam (Ti:sapphire femtosecond oscillator Mai-Tai HP, Spectra-Physics, 80 MHz, 100 fs, 800 nm) was tightly focused into the protein ink by oil immersion (NA = 1.35) lens (60×). Singlet oxygen (1O2) produced after two-photon absorption of RhB and tryptophan (Trp) occurred in the core region, which promotes intramolecular and intermolecular crosslinks of protein residues to form a water-insoluble gel[25,26].

In order to ensure low surface roughness, the laser power was set at 28 mW before the objective lens to induce the crosslinking of protein molecules in the central area of the focal spot after the optimization of processing parameters, and the single exposure time was 1000 μs, while the scan point interval was 100 nm[27]. A piezo stage (Physik Instrumente P-622.ZCD) was used to control the z-direction movement of the laser focus. In the x–y plane, a two-galvano-mirror set was used to control the laser focus scanning[28]. The unreacted protein was removed when the sample was rinsed in water after FsLDW. In this way, the protein MLA was directly custom-made. The fabricated PMLADC was investigated by a scanning electron microscope (SEM, JSM-7500 F, JEOL) and a laser scanning confocal microscope (LSCM, OLS3000, EVC Electronic).

With the help of FsLDW, the PMLADC was successfully prepared, as shown in Fig. 1. The PMLADC was investigated and characterized by scanning electron microscopy; the SEM images were taken from the top

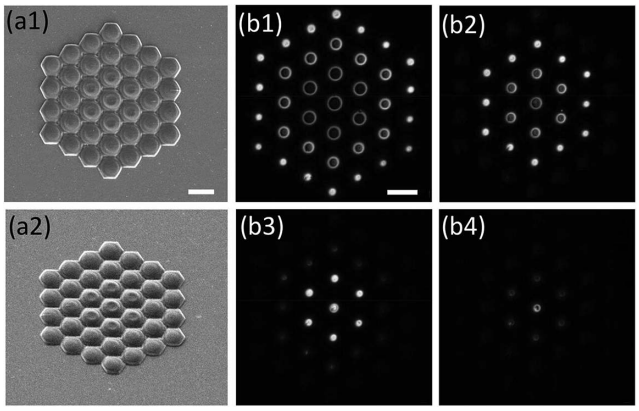

Fig. 1. (a1) and (a2) SEM images of four-circle PMLADC taken from top and 45°, respectively; scale bar: 20 μm. (b1)–(b4) The LSCM images of four-circle PMLADC were taken with 1 μm position interval; scale bar: 20 μm.

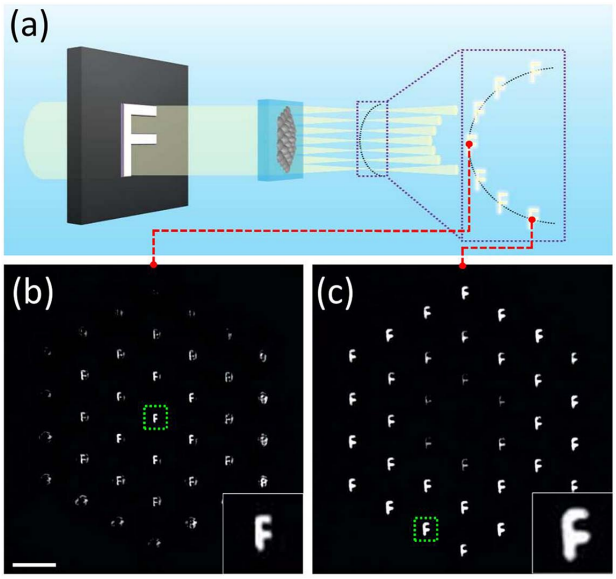

Fig. 2. (a) Schematic of the test of the PMLADC. Imaging pictures were taken at (b) 19.6 μm and (c) 24.2 μm from PMLADC; scale bar: 20 μm.

[Fig. 1(a1)] and 45° [Fig. 1(a2)] directions. The PMLADC was designed to consist of 37 unit lenses; the radii of which were all 10 μm, and the height of the lenses of each circle was 8, 7, 6, and 5 μm from inside to outside, which were experimentally confirmed by an LSCM [Fig. 1(b)]. Of course, the device size is the same as the design size when the scan is completed, but when developed, the actual size will be slightly reduced due to the change from a liquid environment to a dry environment. As shown in Fig. 1(b), all lenses can be observed [Fig. 1(b1)] when the laser is focused at a low position, and with the laser focus moved up, the outer circle ones disappeared gradually [Figs. 1(b2) and 1(b3)]. Finally, only the center lens can be observed [Fig. 1(b4)]. It can be noticed that the lenses in the center of lens array in Fig. 1(a2) had slightly sunk, which was mainly caused by the protein-hydrogel dehydration in vacuum for SEM detection. Then, a simple test system had been built up, which is shown in Fig. 2(a). A tungsten filament bulb was used as light source and passed through a shading plate with a hollow letter F. The letter F worked as an objective and was transformed onto a moveable observation screen by PMLADC. The four-circle PMLADC was designed with four groups of focus, which are located in a curved surface distribution in the space marked with a black dotted line in Fig. 2(a). Imaging pictures were taken at 19.6 and 24.2 μm from the PMLADC in Figs. 2(b) and 2(c), respectively. The lenses in the center and at the edge cannot image clearly simultaneously, because the images of the unit lenses were located on a curve surface not a flat surface.

In order to quantitatively analyze the non-planar focusing characteristics, the one-row PMLADC was designed and fabricated, as shown in Fig. 3(a). The radii of unit lenses were still 10 μm, and the heights of the lenses were 10, 8, 6, 5, 4, and 3 μm from left to right. The focusing characteristics were tested using the optical system in Fig. 2(a) by removing shading plate. When the observation screen moved away from the MLA along the optical axis, the leftmost lens was focused firstly. By continuing to move the observation screen, each lens was focused in turn. Finally, only the two rightmost lenses were focused. The focus images were taken at 18.2, 19.6, 22.7, 26.2, 34.0, and 41.4 μm from the lenses, respectively [Fig. 3(b)]. The light intensity distribution and focusing spot size were extracted from focus images [Fig. 3(c)]. It is obvious that the focusing spot sizes were increased gradually.

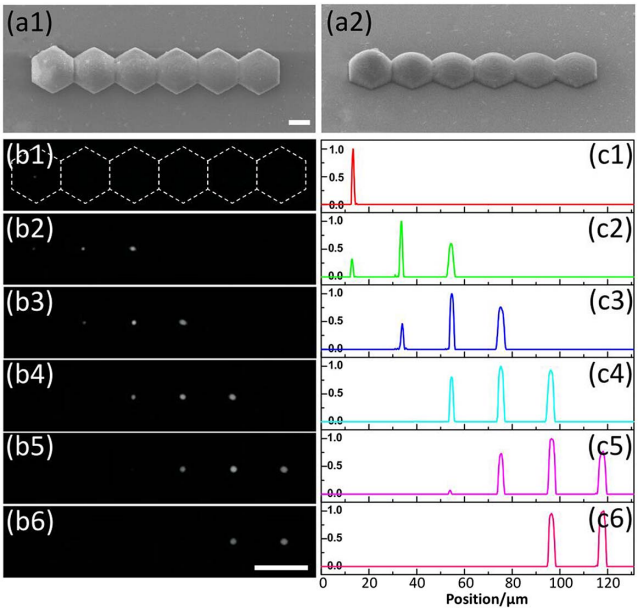

Fig. 3. (a1) and (a2) SEM images of one-row microlenses taken from the top and 45°. (b1)–(b6) Focus images were taken at different locations from the lenses: 18.2 μm, 19.6 μm, 22.7 μm, 26.2 μm, 34.0 μm, 41.4 μm, respectively. (c1)–(c6) Relative intensity distribution of focus images (b1)–(b6). Scale bar: (a) 10 μm, (b) 20 μm.

It is because the numerical aperture of the lenses decreases gradually from left to right, which conforms to the basic laws of physics.

The protein molecule contains a large number of electriferous groups, such as negatively charged carboxyl group and positively charged amino group. When in an aqueous environment, the different degrees of ionization will lead to the expansion and contraction of protein molecules. Therefore, through altering the pH or ion concentration in aqueous solution to change the ionic state of electriferous groups in protein molecules, the equilibrium swelling of protein-hydrogel can be adjusted (stimulated drying shrinkage or water swelling)[29]. Based on excellent quality device and optical performance, by using such characteristics of protein-hydrogel, we can further realize the environmental response dynamic focusing ability of PMLADC. The LSCM image of one-row PMLADC was taken in the solution, as shown in Fig. 4(a). Firstly, the lens group was soaked in inorganic phosphate solution (pH = 7). The expansion and contraction of protein molecules were observed by irregularly altering the pH value, and the corresponding profile lines are shown in Fig. 4(b). When the pH increased from 7.0 to 9.0, all the lenses grew in size after water swelling. The lenses reached the largest size when the pH increased to 11.0. At this point, by reducing the pH back to 7.0, the lenses would shrink. The response is reversible, which makes the device have certain practical application values. The radius of curvature of the spherical lens can be achieved by using a software fitting lens contour line. As shown in Fig. 4(c), the rightmost three lenses A, B, C were fitted. All of the lenses showed the same response to pH in much the same way.

Generally speaking, the decrease of the radius of curvature of the spherical lens will lead to the decrease of the focal length. However, in the process of the pH value dynamic tuning test in our work, we found that the focal length of protein-based spherical microlenses increases with the decrease of radius of curvature induced by pH. Take lens B as an example. As shown in Fig. 4(c), when the pH is 7, the radius of curvature is about 18 μm, and when the pH changes to 3, 9, or 11, the radius of curvature is reduced. We obtained the focal length of lens B with the various pH concentrations in the liquid phase [shown in Fig. 5(a)] by using the test system mentioned in Fig. 2. The focal distance of a protein-based microlens in a water environment conforms to the following formula:

$$f = \frac{n_{aq}}{\frac{n_{hy}-n_{aq}}{r} + \frac{n_{gl}-n_{hy}}{r'}}, \tag{1}$$

where f is the focal length of the lens, and n_{aq}, n_{hy}, n_{gl} are the refractive index of the solution, the protein-hydrogel, and the glass substrate, respectively. The r and r' are the radii of curvature of lens/aqueous solution and lens/glass substrate. As $r' = \infty$, the above formula can be transformed into

$$f = n_{aq} r (n_{hy} - n_{aq}). \tag{2}$$

In the experiment, n_{aq} basically remained at about 1.33; therefore, the corresponding refractive index of protein-hydrogel can be obtained as 1.452, 1.421, 1.459, 1.44, and 1.418, respectively. Which is to say, with the increase or decrease of pH, the protein-hydrogel has water absorption expansion, its effective refractive index n_{hy} decreases, and the effect of n_{hy} is more than the smaller radius of

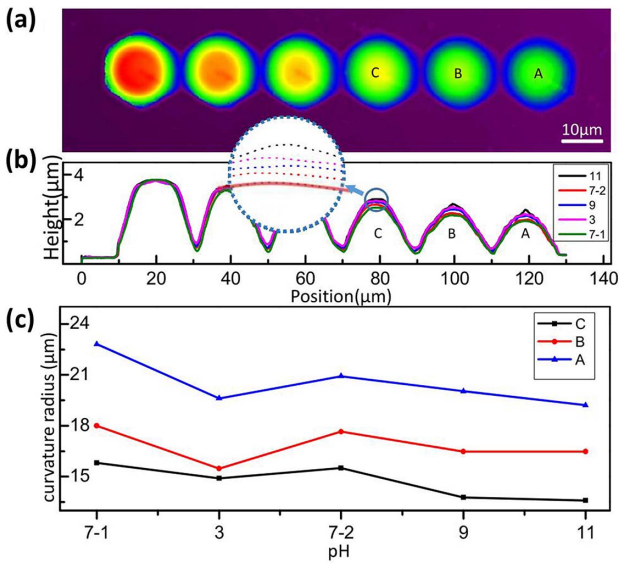

Fig. 4. (a) LSCM images of one-row PMLADC; scale bar: 10 μm. (b) The profile lines of the lens group under different pH values. (c) The curvature radii of lenses A, B, C under different pH values.

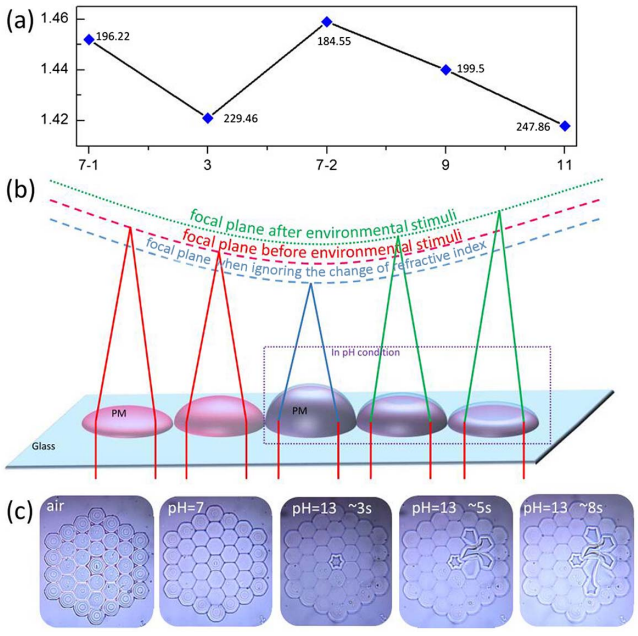

Fig. 5. (a) Focal length and refractive index of lens B at different pH values. (b) Schematic of the change of the focal plane of the one-row PMLADC and (c) schematic of four-circle PMLADC under a microscope.

curvature of the lens. As shown in Fig. 5(b), one-row PMLADC has a fixed focal plane (red line) in the air after the preparation is completed. When the PMLADC was immersed in pH solution, the radius of curvature of the microlens decreases with the equilibrium swelling of protein-hydrogel, and if the n_{hy} remains unchanged, the focal length should be the blue line. However, the focal length we actually measured is the green line. Interestingly, we know that different power can bring a different refractive index of the protein-hydrogel[30]. By using this property, we can easily make the lens groups with more complex and diverse focal planes. It is important to note that when the ion concentration is too high, the lens will rupture due to excessive water absorption [shown in Fig. 5(c)].

We used natural protein material as the main material to form the 3D focal plane lens group by femtosecond laser two-photon polymerization. The focal plane of the lens group has been controlled by using the equilibrium swelling of the protein-hydrogel. The pH value is an important parameter of the physiological process or living environment, as the living environments of all kinds of human bodies, animals, or micro-organisms have their typical pH values. Also, changes in physiological or life activities can cause a corresponding change in the pH value of the environment. Thus, the pH value response dynamic tuning mechanism we use here may have its unique significance for biomedical applications. Therefore, the protein-based spherical microlenses can respond to the pH value dynamically and have great potential in biological sensing, optical integration of microfluidic biochips, and other fields.

The author Zhishan Hou thanks Dr. Yunlu Sun at Jilin University for the guidance. This work was supported by the National Natural Science Foundation of China (NSFC) (Nos. 61605055 and 61435005) and the China Postdoctoral Science Foundation (No. 801161010428).

References

1. S. R. Quake and A. Scherer, Science **290**, 1536 (2000).
2. D. Wu, J. Xu, L. G. Niu, S. Z. Wu, K. Midorikawa, and K. Sugioka, Light: Sci. Appl. **4**, e228 (2015).
3. B. Sasa, P. Mauro, F. Holger, D. Martin, H. N. Chapman, and A. J. Morgan, Light: Sci. Appl. **7**, 17162 (2018).
4. D. Wu, S. Z. Wu, L. G. Niu, Q. D. Chen, R. Wang, J. F. Song, H. H. Fang, and H. B. Sun, Appl. Phys. Lett. **97**, 031109 (2010).
5. T. R. M. Sales, Opt. Eng. **42**, 3084 (2003).
6. N. A. Baharudin, C. Fujikawa, O. Mitomi, A. Suzuki, S. Taguchi, O. Mikami, and S. Ambran, IEEE Photon. Technol. Lett. **29**, 949 (2017).
7. J. Y. Son, B. Javidi, S. Yano, and K. H. Choi, J. Disp. Technol. **6**, 394 (2010).
8. J. Duparré, P. Dannberg, P. Schreiber, A. Bräuer, and A. Tünnermann, Appl. Opt. **43**, 4303 (2004).
9. J. C. Chu, L. Xiang, J. D. Wu, Y. Peng, S. Liu, Q. Yang, and H. Zheng, Opt. Laser Technol. **89**, 92 (2017).
10. F. Y. Lin, L. Y. Chu, Y. S. Juan, S. T. Pan, and S. K. Fan, Proc. SPIE **6584**, 65840D (2007).
11. H. Ren, Y. H. Fan, and S. T. Wu, Appl. Phys. Lett. **83**, 1515 (2003).
12. D. P. Lin, J. H. Zheng, K. Gui, K. N. Wang, and Y. N. Wang, Optik **127**, 7788 (2016).
13. H. Ren, D. Fox, P. A. Anderson, B. J. Wu, and S. T. Wu, Opt. Express **14**, 8031 (2006).
14. Y. L. Sun, W. F. Dong, R. Z. Yang, X. Meng, L. Zhang, Q. D. Chen, and H. B. Sun, Angew. Chem. Int. Ed. **51**, 1558 (2012).
15. W. Xiong, Y. S. Zhou, X. N. He, Y. Gao, M. Mahjouri-Samani, L. Jiang, T. Baldacchini, and Y. F. Leng, Light: Sci. Appl. **1**, e6 (2015).
16. Y. L. Sun, W. F. Dong, L. G. Niu, T. Jiang, D. X. Liu, L. Zhang, Y. S. Wang, D. P. Kim, Q. D. Chen, and H. B. Sun, Light: Sci. Appl. **3**, e129 (2014).
17. Y. L. Zhang, Q. D. Chen, H. Xia, and H. B. Sun, Nano Today **5**, 435 (2010).
18. X. Q. Liu, Q. D. Chen, K. M. Guan, Z. C. Ma, Y. H. Yu, Q. K. Li, Z. N. Tian, and H. B. Sun, Laser Photon. Rev. **11**, 1600115 (2017).
19. Y. L. Zhang, L. Guo, S. Wei, Y. Y. He, H. Xia, Q. D. Chen, H. B. Sun, and F.-S. Xiao, Nano Today **5**, 15 (2010).
20. R. Fang, A. Vorobyev, and C. Guo, Light: Sci. Appl. **6**, e16256 (2017).
21. D. Wu, Q. D. Chen, L. G. Niu, J. N. Wang, J. Wang, R. Wang, H. Xia, and H. B. Sun, Lab Chip **9**, 2391 (2009).
22. D. Yin, J. Feng, R. Ma, Y. F. Liu, Y. L. Zhang, X. L. Zhang, Y. G. Bi, Q. D. Chen, and H. B. Sun, Nat. Commun. **7**, 11573 (2016).
23. D. Dumas, M. Fendler, F. Berger, B. Cloix, C. Pornin, N. Baier, G. Druart, J. Primot, and E. le Coarer, Opt. Lett. **37**, 653 (2012).
24. S. Abrahamsson, J. J. Chen, B. Hajj, S. Stallinga, A. Y. Katsov, J. Wisniewski, G. Mizuguchi, P. Soule, F. Mueller, C. D. Darzacq, X. Darzacq, C. Wu, C. I. Bargmann, D. A. Agard, M. Dahan, and M. G. L. Gustafsson, Nat. Methods **10**, 60 (2012).
25. M. J. Davies, Photochem. Photobiol. Sci. **3**, 17 (2004).
26. H. R. Shen, J. D. Spikes, C. J. Smith, and J. Kopecek, J. Photochem. Photobiol. A: Chem. **130**, 1 (2000).
27. B. B. Xu, Y. L. Zhang, H. Xia, W. F. Dong, H. Ding, and H. B. Sun, Lab Chip **13**, 1677 (2013).
28. H. Xia, J. Wang, Y. Tian, Q. D. Chen, X. B. Du, Y. L. Zhang, Y. He, and H. B. Sun, Adv. Mater. **22**, 3204 (2010).
29. B. Kaehr and J. B. Shear, Proc. Natl. Acad. Sci. USA **105**, 8850 (2008).
30. S. M. Sun, Y. L. Sun, B. Y. Zheng, P. Wang, Z. S. Hou, W. F. Dong, L. Zhang, Q. D. Chen, L. M. Tong, and H. B. Sun, Sens. Actuators B **232**, 571 (2016).